Available online at www.sciencedirect.com
SCIENCE DIRECT
International Journal of Pharmaceutics 310 (2006) 146–153
INTERNATIONAL JOURNAL OF PHARMACEUTICS
www.elsevier.com/locate/ijpharm

Dissolution characteristics of cylindrical particles and tablets

Tadashi Fukunaka [a,*], Yoshiko Yaegashi [b], Taku Nunoko [b], Ryusei Ito [b], Boris Golman [b], Kunio Shinohara [b]

[a] *Banyu Pharmaceutical Co., Ltd. 9-1, Kamimutsuna 3-Chome, Okazaki, Aichi 444-0858, Japan*
[b] *Division of Chemical Process Engineering, Graduate School of Engineering, Hokkaido University, Nishi 8, Kita 13, Kita-ku, Sapporo, Hokkaido 060-8628, Japan*

Received 5 August 2005; received in revised form 21 October 2005; accepted 3 December 2005
Available online 18 January 2006

Abstract

In this paper, dissolution characteristics of primary-particles and compressed tablets were investigated by experiments using a mathematical model. For the primary-particle, it was found that the dissolution rate increased with a decrease in the particle size. Assuming that primary-particles of size distribution were of cylindrical shape and that the dissolution occurs from the total external surface, an extended Nernst–Noyes–Whitney equation fitted to the experimental data well. As the influences of particle size and shape on thickness of a diffusion-boundary film were found to be quite low, the dissolution rate was considered to be affected by the specific surface area dominantly. Furthermore, the same model was applied to a compressed tablet and fitted to the data well. Though the rate constant obtained were not affected by the properties of primary-particles forming the tablet, it was found to increase with the apparent voidage which occupies the inter-particle volume of tablet diluent among less soluble particles. Consequently, an increase in the apparent voidage is presumed to accelerate penetration of water into the internal voids of the tablet. Thus, the dissolution going, the effective surface area inside the tablet is considered to be extended.

Keywords: Dissolution; Mathematical model; Tablet; Particle shape; Particle size; Active pharmaceutical ingredients

1. Introduction

Currently, tablets have been applied extensively to a dosage form of medical drug due to the easy handling for the user and high productivity for the manufacturer. In the pharmaceutical field of formulation design, the dissolution profile is one of the important issues, since most of active pharmaceutical ingredients (APIs) have poor solubility in water.

Though the dissolution characteristics of single particles have been reported extensively by quite a few investigators (Anderberg et al., 1988; Anderberg and Nystrom, 1990; Bisrat et al., 1992; Bisrat and Nystrom, 1988), most of the models have defined the particles as spherical shaped. In contrast, the characteristics of the tablets also have been reported by many investigators (Alway et al., 1996; Goehl et al., 1983; Hendrilsen and Williams, 1991; Ibrahim and Sallam, 1993; Najib and Jalal, 1988; Rost and Quist, 2003). However, most of them have been analyzed experimentally and qualitatively and some models have not considered the geometrical or physical properties of the tablet (shape, voidage, etc.) fully yet.

Furthermore, the effect of particle shape on the dissolution rate has been investigated as well as that of particle diameter (Mosharraf and Nystrom, 1995). However, extensive comparison of the particle shape on the same substance has not been performed fully yet.

In our previous paper (Ito et al., 2005), though the dissolution characteristics of the compressed tablet were investigated, the effects of properties of particles forming the tablet on the dissolution rate were limited due to the simplicity of an applied model by power law.

In this paper, at first, the dissolution characteristics of primary-particles forming the tablet were investigated using an extended Nernst–Noyes–Whitney equation which took into account the cylindrical shape of API and the particle size distribution. Secondary, the model was also applied to the tablet to investigate the influences of the size and the shape of particles forming the tablet and the apparent voidage of the tablet on the dissolution rate.

* Corresponding author. Tel.: +81 564 57 1765; fax: +81 564 57 1766.
E-mail address: tadashi_fukunaka@merck.com (T. Fukunaka).

0378-5173/$ – see front matter © 2005 Elsevier B.V. All rights reserved.
doi:10.1016/j.ijpharm.2005.12.006

Nomenclature

A_1, A_3	coefficients in Eq. (19) (m/s)
A_2	coefficient in Eq. (19)
a, b	minor and major axes of approximate ellipse by shape analysis (m)
C	weight concentration of Ethenzamide (kg/m^3)
D	diffusion coefficient of Ethenzamide in water solution (m^2/s)
d	spherical particle diameter (m)
f	weight distribution density of particles
K_{shape}	shape index of particle
k	dissolution rate constant (m/s)
k_0	dissolution coefficient (s^{-n})
M_{dis}	dissolved amount of Ethenzamide (kg)
m	weight of sample (kg)
p	dissolution exponent
R	dissolution fraction
r	radius of base circle of cylinder (m)
S	surface area of primary-particle (m^2)
t	dissolution time (min)
V	volume (m)
v_{p}	median dissolution rate (s^{-1})
x	average particle diameter (m)

Greek letters

δ	thickness of diffusion film (m)
ε	voidage of tablet
ϕ	fraction of Ethenzamide
ρ	particle density (kg/m)

Subscripts

cyl	cylindrical particle
ETZ	Ethenzamide
Lac	Lactose
n	number of class of particle size distribution
p	primary-particle
res	bulk solution
sat	saturated
sph	spherical particle
T	tablet
v	volume
w	weight

2. Theoretical considerations

2.1. Dissolution model on cylindrical primary-particle

It is assumed that a primary-particle is cylindrical, because most of milled particles are needle shaped from the SEM photograph, as shown in Fig. 1, and, comparing the measured specific surface area with the calculated values for the particle assumed to be cylindrical, rectangular parallelepiped and ellipsoidal shape, the cylindrical ones are the most consistent with actual data. The dissolution is assumed to occur only on the external surface

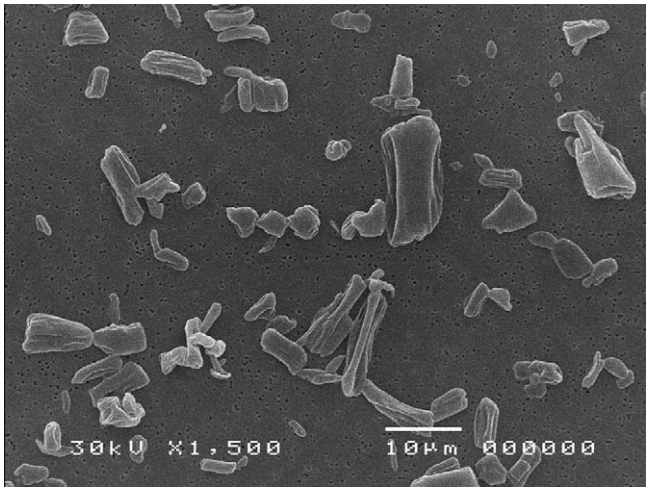

Fig. 1. SEM photograph of Ethenzamide primary-particles.

keeping the same shape based on the experimental observation and the simplification of the model, as shown in Fig. 2.

For a cylindrical particle which belongs to the nth class of particle size distribution, the particle shape index K_{shape} is defined as:

$$K_{\text{shape}} = \frac{a_n}{b_n} \tag{1}$$

where a_n and b_n are the minor and major axes of the particle, respectively. The distribution of shape index is not taken into account.

The volume $V_{\text{p},n}$ and surface area S_n of the particle are expressed using a radius of the base circle of the cylinder as r_n ($=a_n/2$), respectively:

$$V_{\text{p},n} = \pi \frac{a_n^2}{4} b_n = \frac{2\pi r_n^3}{K_{\text{shape}}} \tag{2}$$

$$S_n = 2\pi \frac{a_n^2}{4} + \pi a_n b_n = 2\pi r_n^2 \left(1 + \frac{2}{K_{\text{shape}}}\right) \tag{3}$$

The dissolution rate $\mathrm{d}M_{\text{dis},n}/\mathrm{d}t$ can be expressed by Noyes and Whitney (1897) and Nernst (1904) as:

$$\frac{\mathrm{d}M_{\text{dis},n}}{\mathrm{d}t} = \frac{D}{\delta} S_n (C_{\text{sat}} - C_{\text{res}}) = k_{\text{p}} S_n (C_{\text{sat}} - C_{\text{res}}) \tag{4}$$

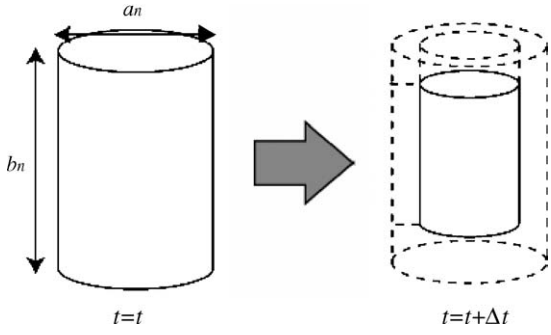

Fig. 2. Dissolution model for cylindrical primary-particle.

where t is the dissolution time, D the diffusion coefficient, δ the thickness of diffusion film, C_{sat} the saturated concentration of API, C_{res} the bulk concentration of API in a vessel and k_p is the dissolution rate constant.

On the other hand, the relationship between the amount of dissolution and the particle volume is given as:

$$dM_{dis,n} = -\rho_p \, dV_{p,n} \tag{5}$$

where ρ_p is the true density of API particle.

Substitution of Eq. (5) into the left-hand side of Eq. (4) gives the related equation of the radius with the dissolution time as follows:

$$\frac{dM_{dis,n}}{dt} = -\rho_p \left(\frac{6\pi}{K_{shape}} r_n^2 \right) \frac{dr_n}{dt} \tag{6}$$

Substitution of Eqs. (3) and (6) into Eq. (4) leads to the related equation of the representative radius with the dissolution time as follows:

$$\frac{dr_n}{dt} = -\frac{k_p}{3\rho_p}(K_{shape} + 2)(C_{sat} - C_{res}) \tag{7}$$

On the dissolution of the particle belonging to the nth class of the particle size distribution, the bulk concentration is written by using Eq. (2) as:

$$C_{res} = \frac{M_{dis,n}}{V_{res}} = \frac{2\pi\rho_p(r_{n,0}^3 - r_n^3)}{K_{shape} V_{res}} \tag{8}$$

where $r_{n,0}$ is the initial radius of the base circle of the cylindrical particle and V_{res} is the volume of bulk solution.

Substitution of Eq. (8) into Eq. (7) gives the variation of the radius with dissolution time as:

$$\frac{dr_n}{dt} = -\frac{k_p}{3\rho_p}(K_{shape} + 2)\left(C_{sat} - \frac{2\pi\rho_p(r_{n,0}^3 - r_n^3)}{K_{shape} V_{res}} \right) \tag{9}$$

Furthermore, a dissolution fraction at time t is defined as:

$$R \equiv \frac{M_{dis,n}(t)}{M_{dis,n}(\infty)} = \frac{\rho_p(V_{p,n}(0) - V_{p,n}(t))}{\rho_p(V_{p,n}(0) - V_{p,n}(\infty))} = \frac{V_{p,n}(0) - V_{p,n}(t)}{V_{p,n}(0)} = \frac{r_{n,0}^3 - r_n(t)^3}{r_{n,0}^3} \tag{10}$$

where $V_{p,n}(\infty)$ could be regarded as nearly zero.

2.2. Dissolution model for cylindrical particles with size distribution

Taking the particle size distribution into account, the concentration of bulk solution can be expressed as:

$$C_{res} = \sum_n \frac{M_{dis,n} f(r_n) \Delta r_n}{V_{res}} = \sum_n \frac{\rho_p(V_{p,n}(0) - V_{p,n}(t)) f(r_n) \Delta r_n}{V_{res}} = \sum_n \frac{2\pi\rho_p}{K_{shape} V_{res}} (r_{n,0}^3 - r_n^3) f(r_n) \Delta r_n \tag{11}$$

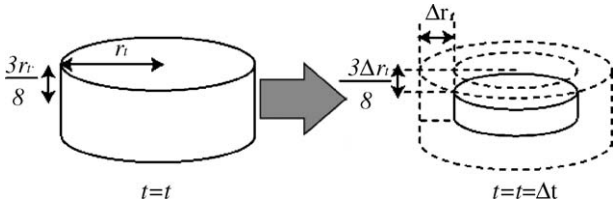

Fig. 3. Dissolution model for compressed tablet.

where $f(r_n)\,\Delta r_n$ is the weight fraction belonging to the nth class of particle size distribution. Substituting Eq. (11) into Eq. (7), the variation of the radius with dissolution time is obtained. Here, the dissolution fraction, R, at time, t is defined as:

$$R \equiv \frac{\sum_n M_{dis,n}(t)}{\sum_n M_{dis,n}(\infty)} = \frac{\sum_n (r_{n,0}^3 - r_n(t)^3)}{\sum_n r_{n,0}^3} \tag{12}$$

2.3. Dissolution model for compressed tablet

Assuming that the dissolution is performed only from the external surface while keeping the same shape, as shown in Fig. 3, the rate is followed by Eq. (7), and that C_{res} is much smaller than C_{sat}, substitution of r_T and k_T into $r_{n,0}$ and k_p gives:

$$\frac{dr_T}{dt} = -\frac{k_T}{3\rho_p}(K_{shape} + 2)C_{sat} \tag{13}$$

where r_T and k_T denote the radius of base circle and the dissolution rate constant of the tablet, respectively.

Furthermore, the dissolution fraction at time t is defined as:

$$R = \frac{r_{T,0}^3 - r_T(t)^3}{r_{T,0}^3} \tag{14}$$

3. Materials and methods

3.1. Dissolution sample

Ethenzamide (ETZ) particles ($C_9H_{11}NO_2$: 165.19, 1.25 g/cm^3, Iwaki Seiyaku Co., Ltd.) milled by means of a fluidized-bed jet-mill (Hosokawa Micron Corp. Counter Jet-mill 100 AFG) are used as a model API, and the properties of milled particles are listed in Table 1. Lactose (Lac) particles ($C_5H_{12}O$: 342.3, 1.58 g/cm^3, Wako Pure Chemical Industries, Ltd.) are also used as a tablet diluent.

Table 1
Sample properties

Sample no.	Average particle diameter, x (μm)	Shape index, K_{shape}
1	8.177	0.590
2	9.989	0.544
3	16.22	0.567
4	16.24	0.606
5	17.02	0.626
6	30.33	0.619

3.2. Shape analysis of milled Ethenzamide

Particle shape analysis (Fukunaka et al., 2005) was performed by Fourier transformation of each point on the circumference of the projected particle image on rectangular coordinates, after a SEM photograph of the particle sample was first digitized and then binarized to extract the particle outline using image analysis software, Optimas (Media Cybernetics, version 6.5). The shape index of each particle was calculated as the ratio of minor- to major-axis of the approximate ellipse which is obtained by the shape analysis. The representative shape index K_{shape} of the sample in this paper is the value of 50% passage fraction of the particle shape distribution consisting of 250–330 particles.

3.3. Dissolution test for primary-particle

Three hundred milliliters of distillated water with 1 ml of Tween 20 (Kanto Chemical Co., Inc.) as a dispersant was put in a glass beaker kept at $37 \pm 0.5\,^{\circ}C$ in a thermostatic bath and agitated with a magnetic stirrer vigorously. 0.2 g of primary-particles were thrown into the solution and dissolved. Sampling was carried out by collecting 0.8 ml of the sample solution at a given period.

3.4. Preparation of compressed tablet

A compressed tablet 8 mm in diameter and 3 ± 0.015 mm in thickness was prepared by utilizing a mold and a testing stage set on a pedestal of a uni-axial compression apparatus (JMT-42A, JACOM). The voidage of the tablet ε was adjusted by changing the filling weight of the sample m to mold the tablet of prescribed volume V. The void fraction is calculated by the following equation:

$$\varepsilon = 1 - \frac{m}{\rho_{ETZ} V} \tag{15}$$

where ρ_{ETZ} is the true density of Ethenzamide.

On the other hand, in the case of mixture of Lactose and Ethenzamide, the overall voidage was calculated as:

$$\varepsilon = 1 - \frac{(m\phi_w/\rho_{ETZ}) + (m(1-\phi_w)/\rho_{Lac})}{V} \tag{16}$$

where ρ_{Lac} is the true density of Lactose and ϕ_w is the weight fraction of Ethenzamide.

Furthermore, regarding Lactose as apparent void, the voidage of Ethenzamide particles was calculated as:

$$\varepsilon_{app} = 1 - \frac{m\phi_w}{\rho_{ETZ} V} \tag{17}$$

3.5. Dissolution test for compressed tablet

Twelve hundred millileters of distillated water was put in a glass beaker, kept at $37 \pm 0.5\,^{\circ}C$ in a thermostatic bath, and agitated by a mechanical stirrer at 300 rpm. The beaker was kept isolated to prevent evaporation during the test. One tablet was put in a metallic cage and dipped into the solution. Sampling was carried out by collecting 1.5 ml of the solution at a given period and the same volume of distillated water was added to keep the liquid volume after sampling.

3.6. Determination of dissolved fraction

Bulk concentration was measured at 290 nm of wavelength by means of HPLC with an ultraviolet spectrum detector (LC-VP series, SHIMADZU Corp.). The dissolved fraction R at t was defined as the ratio of bulk concentrations to the final maximum one as:

$$R = \frac{\text{bulk concentration at } t}{\text{bulk concentration at } t = \infty} \tag{18}$$

4. Results and discussion

4.1. Dissolution characteristics of primary-particle

Fig. 4 shows the dissolution curves of the primary-particles which have various shape indexes and average particle diameters. X and Y axes indicate dissolution time and dissolved fraction, respectively. It seems that smaller particles indicate faster dissolution rate. The particle size distribution was taken into account when the solid lines in Fig. 4 were calculated. The ordinary differential equations resulting from the combination of Eqs. (7), (11) and (12) were solved numerically and the dissolution rate constant was the only free parameter to fit. Since all the R^2 values calculated for the indices of goodness of fit were more than 0.953, the proposed dissolution model on cylindrical particles is considered to be appropriate.

Figs. 5 and 6 show the effects of shape index and average particle diameter on the dissolution rate constant in Eq. (7) which are obtained by curve fitting. As the rate constant was found not to be affected by these two parameters, the effects of particle size and shape on thickness of diffusion film around the particles were negligibly thin. Consequently, it is considered that the dissolution rate is influenced mainly by the specific surface area.

Fig. 7 shows the variation of surface area ratio of cylindrical to spherical particle of the same volume with the shape index. The

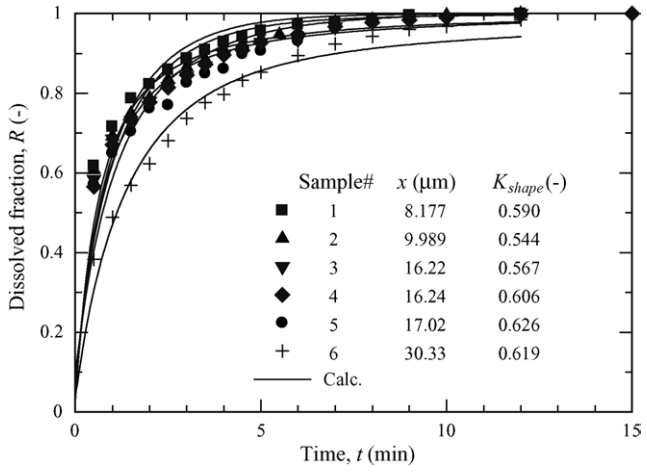

Fig. 4. Dissolution curves with primary-particles.

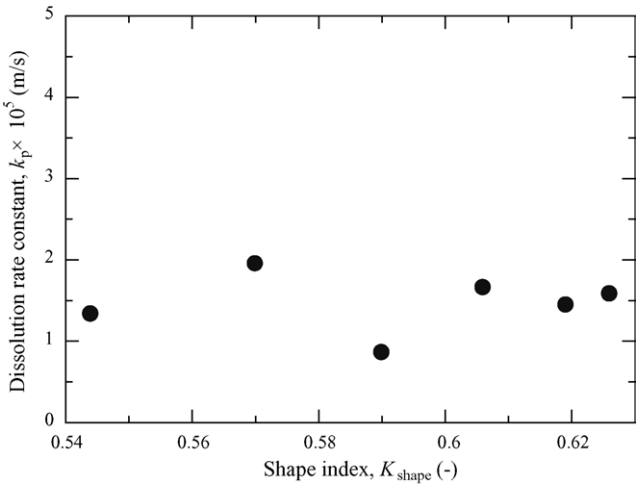

Fig. 5. Effect of shape index on dissolution rate constant.

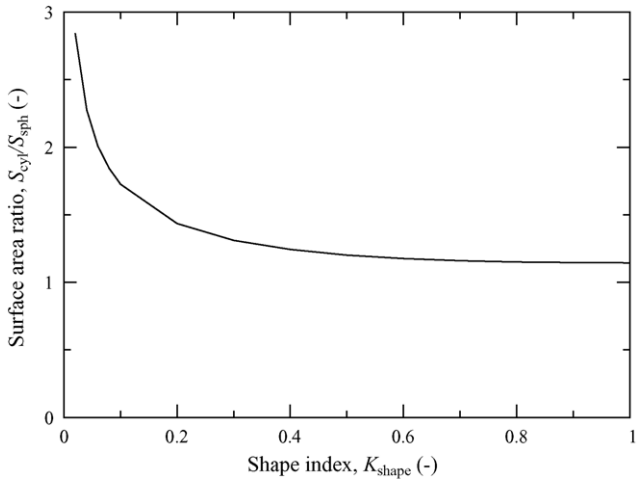

Fig. 7. Variation of surface area ratio of cylindrical to spherical particle of same volume with shape index.

derivation is described in Appendix A. It is found that the ratio is bigger than unity for any value of shape index. As the result, the dissolution rate of primary-particle increases with elongation of cylindrical one.

Fig. 8 shows the effect of average particle diameter on the median dissolution rate v_p which is defined as the dissolution rate dR/dt at 50% fraction of the dissolution curve. It is reasonable to regard that the median dissolution rate increases with decrease in particle size within the experimental error.

In fact, the particle shape index will increase with decrease in particle size by fluidized-bed jet-milling (Fukunaka et al., 2005). Though they are opposite in the trends of the effects on the dissolution rate, the particle size is considered to be more influential than the particle shape.

4.2. Dissolution characteristics of compressed tablet

4.2.1. Effect of primary-particle properties on dissolution rate constant

Figs. 9 and 10 show the dissolution curves of compressed tablets of Ethenzamide particles only and of the mixture of ETZ and Lac particles, respectively. The volumetric fraction of ETZ, ϕ_v, in the mixture was 0.7. In both graphs, it was found that the dissolution rate of the tablet was not affected by the properties of primary-particle. The solid lines indicate the calculated ones from Eqs. (13) and (14) by substitution of 8/3 into K_{shape} for the tablet, which well fit to the experimental data. The dissolution rate constant was the only free parameter to fit and all the R^2 values calculated for the indices of goodness of fit were more than 0.993. In the later stages of dissolution of the mixture tablets in Fig. 10, however, the calculated lines are not consistent with the data slightly as compared with that of ETZ only due to their collapse.

Fig. 11(a and b) show the effects of shape index and average particle diameter on the dissolution rate constant of the tablet in Eq. (13) obtained by curve fitting. The rate constant was found to be affected not by these two parameters, but by the apparent voidage of the tablet as ETZ structure. Though, apparently, this result seems to be contradictory to our previous one (Ito et al., 2005) that particle shape has affected the dissolution coefficient k_0, it is considered to be due to inclusion of the effective surface area, depending on the particle shape, in the overall dissolution rate equation as $k_0 t^p$, as discussed below.

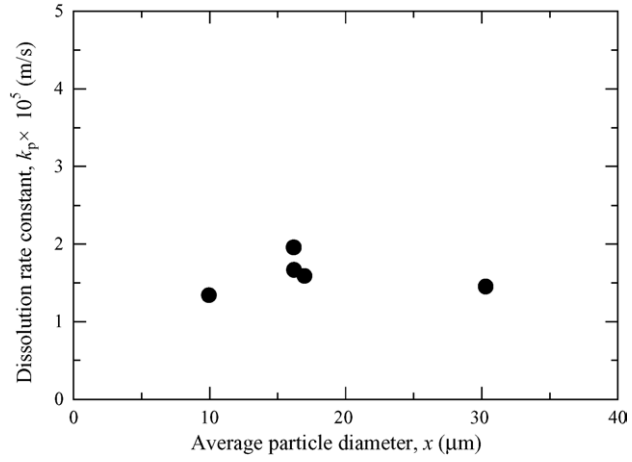

Fig. 6. Effect of average particle diameter on dissolution rate constant.

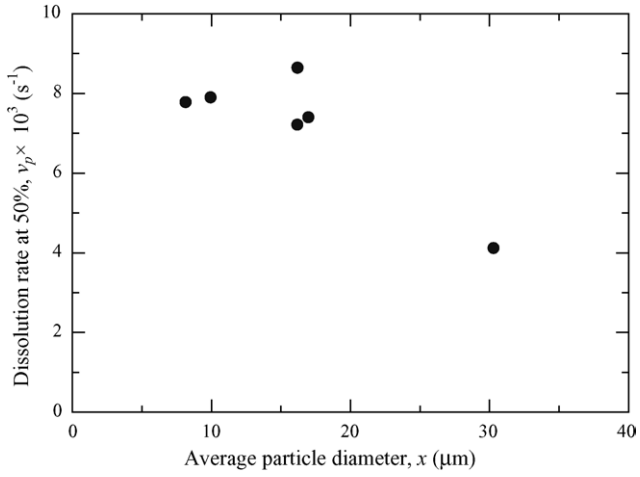

Fig. 8. Effect of average particle diameter on dissolution rate.

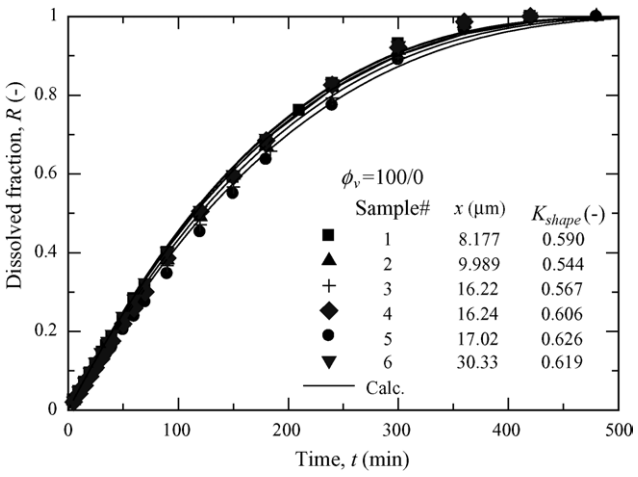

Fig. 9. Effects of primary-particle properties on dissolution curves of tablet (ETZ:Lac = 100:0).

4.2.2. *Effect of voidage of tablet on dissolution rate constant*

To confirm the effect of voidage on dissolution rate constant, the additional tests were performed with tablets which have higher apparent voidage by increasing the volumetric fraction of Lac. Fig. 12 shows the results of the tests including those of previous runs. It was found that higher apparent voidage leads to faster dissolution rate. As the calculated lines well fit to experimental data, the proposed cylindrical model can be applied to the dissolution of compressed tablet. Consequently, in the case of the tablet, it is considered that the dissolution progresses on the basis of the external surface. But, Fig. 13 shows the effect of the apparent voidage occupied with Lac on the dissolution rate constant. It was found that higher voidage yields larger value of the rate constant. To estimate the influence of the apparent voidage, ε_{app} on the rate constant, a regression analysis was applied using a following equation for the rate constant of the tablet due to the voidage as a variable.

$$k_T = A_1 \varepsilon_{app}^{A_2} + A_3 \quad (19)$$

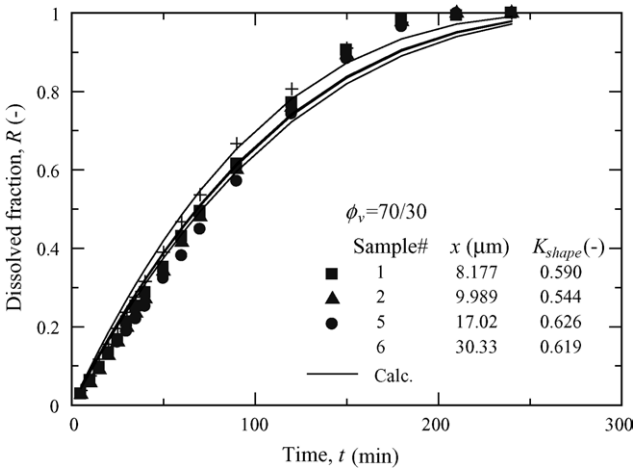

Fig. 10. Effects of primary-particle properties on dissolution curves of tablet (ETZ:Lac = 70:30).

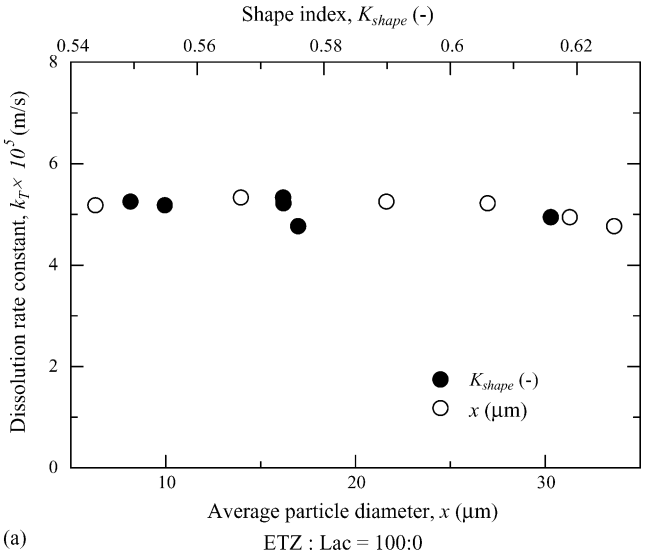

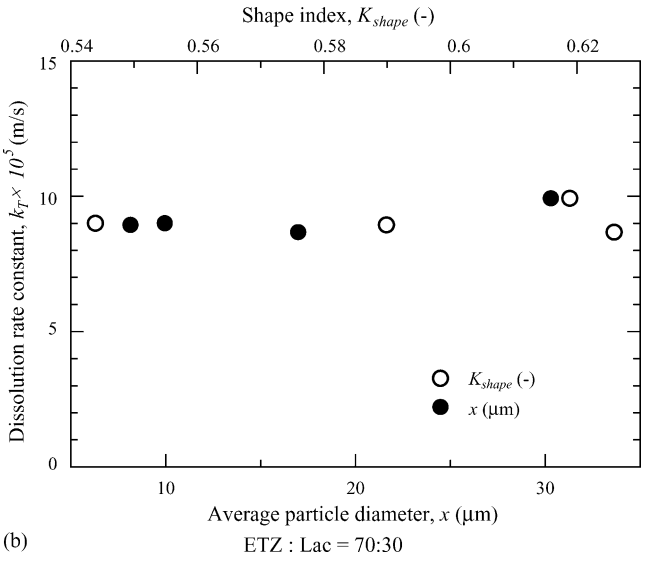

Fig. 11. Effects of primary-particle properties on dissolution rate constant of tablet: (a) ETZ:Lac = 100:0 and (b) ETZ:Lac = 70:30.

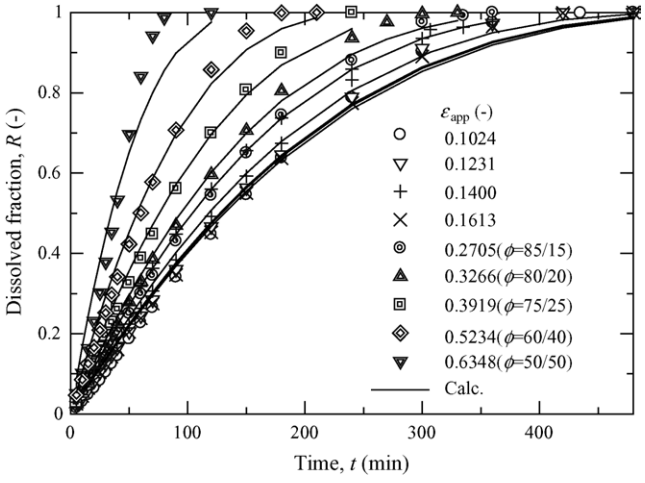

Fig. 12. Effect of apparent voidage of tablet on dissolution curve with sample #5 particles.

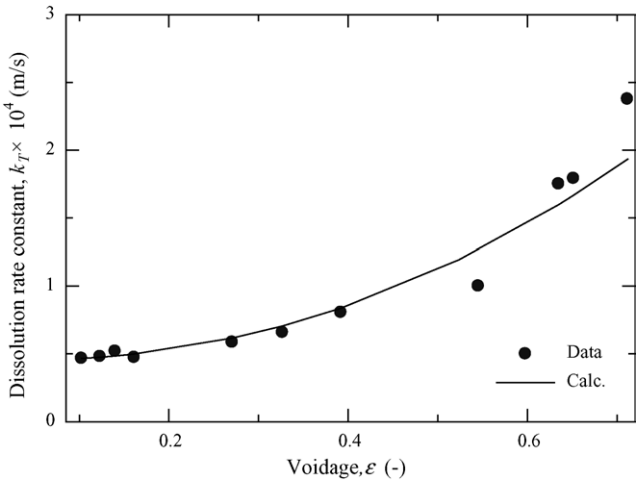

Fig. 13. Effect of apparent voidage on dissolution rate constant of tablet.

As the result, the values of coefficients were obtained as follows:

$$A_1 = 3.1842 \times 10^{-4}\,\text{m/s}, \quad A_2 = 2.2367,$$
$$A_3 = 4.457 \times 10^{-5}\,\text{m/s}$$

Since Eq. (19) is correlated with the data, the dissolution rate constant is considered to depend on the apparent voidage largely. It is presumed that the penetration of water into the tablet is accelerated by an increase in apparent voidage through Lac of faster dissolution. Consequently, as the dissolution progresses, the effective surface area for the dissolution is considered to be extended including internal ETZ particles through the Lac region and partly due to collapse of the tablet.

5. Conclusions

Dissolution characteristics of primary-particles and compressed tablets were investigated. As the result, the following findings were made.

For the primary-particles, smaller particles yield faster dissolution rate. The influences of particle size and shape on the thickness of diffusion film were relatively small. Consequently, the dissolution rate was affected by the specific surface area mainly. As calculated lines fitted to experimental data well, the proposed dissolution model of the cylindrical particles is considered to be appropriate.

For the compressed tablet, it was found that the dissolution rate was not affected by the size and the shape of primary-particle forming the tablet. The rate constant was affected not by these two parameters, but by the apparent voidage of tablet occupied with Lactose particles. As the calculated lines based on the proposed model well fitted to experimental data, it is considered that the dissolution is performed on the external surface of similar shape mainly. On the other hand, as the voidage increases, the penetration of water into the tablet is accelerated due to faster dissolution of Lactose region and partly collapse of the tablet. Consequently, the effective surface area for dissolution is considered to be extended during the dissolution.

Acknowledgements

Many thanks to Mr. Masanao Miyazaki at Pharmaceutical R&D of Banyu Pharmaceutical Co., Ltd. for advice in the dissolution tests. Miss Risa Itoh evaluated the effect of particle shape on the specific surface area.

Appendix A. Derivation of equation of surface area ratio of cylindrical to spherical particle with shape index

Spherical particle volume V_{sph} and surface area S_{sph} of diameter d are given as:

$$V_{\text{sph}} = \frac{4}{3}\pi\left(\frac{d}{2}\right)^3 = \frac{1}{6}\pi d^3 \tag{A.1}$$

$$S_{\text{sph}} = 4\pi\left(\frac{d}{2}\right)^2 = \pi d^2 \tag{A.2}$$

Shape index of cylindrical particle which has a diameter a and a length b is defined as:

$$K_{\text{shape}} = \frac{a}{b} \tag{A.3}$$

The volume V_{cyl} of a cylinder is given as:

$$V_{\text{cyl}} = \left(\frac{a}{2}\right)^2 \pi b = \frac{a^2 b}{4}\pi \tag{A.4}$$

When (A.4) is equivalent to (A.1):

$$a = d\sqrt[3]{\frac{2}{3}K_{\text{shape}}} \tag{A.5}$$

The surface area S_{cyl} of a cylinder is also given as:

$$S_{\text{cyl}} = \frac{a^2}{2}\pi + \pi ab = \pi d^2\left(\frac{2}{3}K_{\text{shape}}\right)^{2/3}\left(\frac{1}{2} + \frac{1}{K_{\text{shape}}}\right) \tag{A.6}$$

Division of (A.6) by (A.2) gives:

$$\frac{S_{\text{cyl}}}{S_{\text{sph}}} = \left(\frac{2}{3}K_{\text{shape}}\right)^{2/3}\left(\frac{1}{2} + \frac{1}{K_{\text{shape}}}\right) \tag{A.7}$$

Consequently, plots of (A.7) with shape index give Fig. 7.

References

Alway, B., Sangchantra, R., Stewart, P.J., 1996. Modeling the dissolution of diazepam in lactose interactive mixtures. Int. J. Pharm. 130, 213–224.

Anderberg, E.K., Bisrat, M., Nystrom, C., 1988. Physicochemical aspects of drug release. VII. The effect of surfactant concentration and drug particle size on solubility and dissolution rate of felodipine, a sparingly soluble drug. Int. J. Pharm. 47, 67–77.

Anderberg, E.K., Nystrom, C., 1990. Physicochemical aspects of drug release. X. Investigation of the applicability of the cube root law for characteri-

zation of the dissolution rate fine particulate materials. Int. J. Pharm. 62, 143–151.

Bisrat, M., Anderberg, E.K., Barnett, M.I., Nystrom, C., 1992. Physicochemical aspects of drug release. XV. Investigation of diffusional transport in dissolution of suspended, a sparingly soluble drug. Int. J. Pharm. 80, 191–201.

Bisrat, M., Nystrom, C., 1988. Physicochemical aspects of drug release. VIII. The relation between particle size and surface specific dissolution rate in agitated suspensions. Int. J. Pharm. 47, 223–231.

Fukunaka, T., Sawaguchi, K., Golman, B., Shinohara, K., 2005. Effect of particle shape of active pharmaceutical ingredients prepared by fluidized-bed jet-milling on cohesiveness. J. Pharm. Sci. 94, 1004–1012.

Goehl, T.J., Sundaresan, G.M., Prasad, V.K., 1983. Studies on the dissolution characteristics of norethindrone–mestranol tablets. Int. J. Pharm. 15, 115–123.

Hendrilsen, B.A., Williams, J.D., 1991. Characterization of calcium fenoprofen: 2. Dissolution from formulated tablets and compressed rotating discs. Int. J. Pharm. 69, 175–180.

Ibrahim, H.G., Sallam, E., 1993. Dissolution from disintegrating tablet: separate contributions from granules and primary drug particles considered. Int. J. Pharm. 93, 111–120.

Ito, R., Nishimura, M., Golman, B., Shinohara, K., Fukunaka, T., 2005. Dissolution characteristics of compressed tablets. Kagaku Kogaku Ronbunshu 31, 1–4.

Mosharraf, M., Nystrom, C., 1995. The effect of particle size and shape on the surface specific dissolution rate of microsized practically insoluble drugs. Int. J. Pharm. 122, 35–47.

Najib, N., Jalal, I., 1988. Correlation between dissolution and disintegration rate constants for acetaminophen tablets. Int. J. Pharm. 44, 43–47.

Nernst, W., 1904. Theorie der reaktionsgeschwindigkeit in heterogenen systemen. Z. Phys. Chem. 47, 52–55.

Noyes, A., Whitney, W., 1897. The rate of solution of solid substances in their own solutions. J. Am. Chem. Soc. 19, 930–934.

Rost, M., Quist, P.O., 2003. Dissolution of USP prednisone calibrator tablets. Effects of stirring conditions and particle size distribution. Pharm. Biomed. Anal. 31, 1129–1143.